Reducing Edge Effects in the Classification of High Resolution Imagery

Guiyun Zhou and Nina S.-N. Lam

Abstract

Edge effects have been a problem in image classification especially when scale-based textural methods were included in the classification process. This paper proposes a new approach to reducing edge effects. The essence of the new approach is that all pixels in a moving window make use of the textural information instead of only the center pixel as in the traditional moving window method. The performance of the new approach was tested in three classification scenarios. The results show that the new approach generally produced higher accuracy with larger window size and was much less affected by the edge issues than the traditional moving window method. The new approach yields satisfactory results as long as the window size is smaller than the land-use polygons and the class boundaries are not too complex.

Introduction

Texture information has long been employed to improve the classification accuracy of remotely sensed imagery (Hsu, 1978; Gong and Howarth, 1992; St-Onge and Cavayas, 1995; Jensen, 2005). As image resolution increases, land-use classes become more and more heterogeneous, and the statistical distributions of the pixel values become seldom normal. This has made traditional spectral-based classifiers such as the maximum-likelihood classifier yield unsatisfactory results, as it violates their assumptions such as the multivariate normal distribution (Haack *et al.*, 1987; Chen *et al.*, 2004).

The incorporation of textural information in the mapping and classification process using the traditional moving window method brings about new problems (Ferro and Warner, 2002). Large windows produce stable textural measures but large edge effects as well. Small windows have reduced edge effects but less stable textural measures. The trade-off between edge effect and window size is hard to be predetermined. The edge issue is blamed for most of the classification errors (Maillard, 2003; Warner and Stelnmaus, 2005; Pearlstine *et al.*, 2005). As a result, many researchers avoided the edge pixels in accuracy assessment, and an overly optimistic result might be obtained (Ferro and Warner, 2002).

Studies to find the optimum window size prior to image classification have been going on for a long time and contradictory results were reported in the literature. Nellis and Briggs (1989) suggested that small window sizes might be appropriate in complex landscapes and large window sizes in homogeneous landscapes. Marceau *et al.* (1990), in a study using SPOT imagery, found that the window size that maximized the classification accuracy depended on each specific land-use class and the average window sizes of 17×17 (340 m by 340 m) and 25×25 (500 m by 500 m) achieved satisfactory classification accuracy for more than one land-use type. Gong *et al.* (1992) indicated that windows larger than 7×7 (140 m by 140 m) yielded unsatisfactory classification accuracy using SPOT images. Gong and Howarth (1992) found that the optimum window size depended on the land-use classes studied. Clearly, using the traditional moving window method, the optimum window size depends on many factors, including pixel resolution, size of land-use polygons, and the homogeneity of land-use classes. Despite the above studies, there are no set rules on how to determine the optimal window size prior to image classification (Hodgson, 1998). Gong (1994) used a simple thresholding and region-growing techniques to reduce edge effects. Maillard (2003) suggested extracting edges prior to classification.

Besides the supervised moving-window method, another approach that incorporates textural information in the classification is the split-and-merge segmentation algorithms (Haralick and Shapiro, 1985; Ojala and Pietikäinen, 1999; Ojala *et al.*, 2002; Hu *et al.*, 2005; Lucieer and Stein, 2005; Lucieer *et al.*, 2005). The performance of these algorithms depends on the textural measures, various parameters, and the complexity of the images. These algorithms recursively divide an image into homogeneous regions based on textural measures. To have stable textural measures, these algorithms usually impose a minimum size on the sub-blocks and then apply a boundary-refining procedure, which improve the accuracy of the boundaries to some degree.

From a cognitive perspective, Hodgson (1998) found that classification accuracy from visual analysis conducted by human interpreters increased monotonically with increasing window size, unaffected by edge effects present in purely automated classification. This paper presents a new, automated approach to reducing edge effects in image classification. In this paper, the edge effect refers to the inaccurate or undefined class membership for the pixels

Guiyun Zhou is with Gannett Fleming Inc./GeoDecisions, 4227 Earth City Expressway South, Suite 160, St. Louis, MO 63045 and formerly with the Department of Geography and Anthropology, Louisiana State University, Baton Rouge, Louisiana (gzhou1@lsu.edu).

Nina S.-N. Lam is with the Department of Environmental Sciences, Louisiana State University, Baton Rouge, Louisiana 70803.

Photogrammetric Engineering & Remote Sensing
Vol. 74, No. 4, April 2008, pp. 431–441.

0099-1112/08/7404–0431/$3.00/0

located near the edge of an image or along the class boundaries within an image. In general, large window size has large edge effects. The performance of the new approach was compared with the traditional moving window approach in three classification scenarios.

The New Approach

In the traditional method, a moving window of size $m \times n$ (usually $m = n$) is centered on each pixel and textural measures are computed from this window. The class membership of the center pixel is then decided based on a classification rule. Pixels close to the edges of two or more classes tend to be misclassified because of the confusion caused by mixed classes in the window. One problem with the traditional method is that information collected from the entire moving window is only useful to the center pixel and is not utilized by other pixels in the window. In the new approach, for each window, similarity indices are calculated between the textural measures of the window and the textural measures of the training samples of all target classes. The similarity index measures the degree of similarity between two sets of textural measures. All pixels in the window will utilize the information and record the highest similarity index and its corresponding target class. Each pixel, except those near the border, gets $m \times n$ highest similarity indices since it is included within $m \times n$ windows. From the $m \times n$ similarity indices, each pixel will record the highest one and its corresponding class. As shown below, possible similarity indices include the probability density if the maximum-likelihood classifier is used and the negative or the inverse of the distance if the minimum-distance classifier is used.

Note that in this new method, all pixels in a window obtain the same highest similarity index from that particular window. Thus, after being included and processed in $m \times n$ overlapping windows, a pixel close to the class boundary will be more likely to get the highest similarity index from a window completely located within the class it really belongs to. This will surely mitigate the edge effects considerably. This is illustrated in Figure 1, in which the center pixel (the black point) is close to the boundary between class A and class B. If the traditional moving window method is used, the pixel will be classified based on texture within window 2 only. Since window 2 contains two classes, error and confusion are likely to arise. But with the proposed method, the pixel will have a much higher chance of being correctly classified into class A since it is included in window 1 and texture in window 1 will have a better chance of being correctly categorized as class A texture because window 1 contains only class A texture.

The assumption underlying the new approach is that texture containing mixed classes of pixels is dissimilar to texture containing only one class. The idea comes from the way human image interpreters deal with boundaries. Humans recognize the dissimilarity between texture containing mixed classes and texture containing one single class, and a pixel close to the boundary is classified by humans based on its surrounding homogenous texture instead of by its surrounding window which may cover two or more classes.

The new approach differs from the traditional method only in the way the similarity index computed from a window is used. It requires no change in a classifier since the comparison based on a similarity index is already included in most classifiers. The method does not involve thresholding either, which has to be decided subjectively.

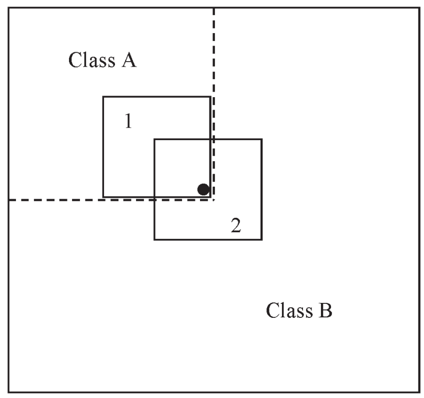

Figure 1. Illustration of the edge effects. The pixel (black point) is highly likely to be misclassified using the textural measures in window 2 as it is the center pixel, whereas it has a much better chance of being correctly classified if window 1 is used. The dashed line is the class boundary.

A Worked Example

Figure 2 shows a worked example to better illustrate the proposed approach using the minimum-distance classifier. The larger the distance, the more dissimilar between textural measures of a window and textural measures of a class. Therefore, for the new approach, the similarity index is chosen as the negative of the distance. Figure 2a is a 6×6 image with three three-uniform classes distinguished by their pixel values 1, 3, and 5. The three classes are referred to as class 1, class 3, and class 5, respectively. The mean values of the three classes are used as the textural measure to discriminate among them. The mean values of a 3×3 moving window, rounded to one decimal point, are shown in Figure 2b. Figure 2c is the classified image by the traditional moving window method using the minimum-distance classifier. Four edge pixels, two of which belonging to class 1 and two of which belonging to class 5, are misclassified as class 3 pixels. Also note that the pixels on the border of the image are not classified because there is no window which is centered on them, and also falls entirely within the image. Using the new approach, when the moving window is centered at position (2, 2), i.e., the second row and the second column, the window has a mean value of 1, and the mean value is closest to class 1. Therefore, the window obtains from class 1 its highest similarity index of 0, which is the negative of the distance. All nine pixels are assigned this similarity index, as shown in Figure 2d. Since none of them is assigned a similarity index before, there is no comparison in this step. When the window moves to position (2, 3), the window has a mean of 2.3 and the mean is closest to class 3. Therefore, the window obtains from class 3 its highest similarity index of −0.7, which is the negative of the distance. After comparison, the six pixels, which fall within both the current window and the previous window and already have a similarity index of 0, keep 0 as their similarity indices since 0 is larger than −0.7. The remaining three pixels in the current window obtain their similarity indices of −0.7 from class 3. Figure 2d also shows the intermediate results when

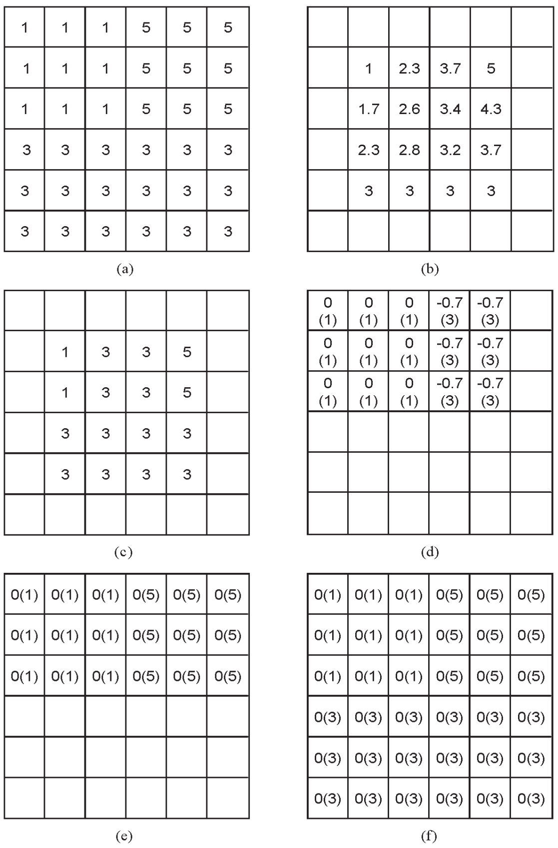

Figure 2. A worked example of the proposed method using a 3×3 moving window: (a) a 6×6 image with three uniform classes (class 1, class 3, and class 5), (b) the image showing the averages of the moving window, (c) classified image using minimum distance classifier by traditional moving window method, (d) the intermediate results of the maximum similarity indices with corresponding class in parentheses after the window moves to row 2 and column 4, (e) the intermediate results after the window moves to row 2 and column 5, and (f) the final results of the new approach.

the window moves to position (2, 4). Figure 2e shows the intermediate results after the window moves to position (2, 5). The window has a highest similarity index of 0 with class 5. After comparison, the six pixels, which fall within both the current window and the previous window and already have a similarity index of -0.7 from class 3, obtain new similarity index of 0 from class 5 since 0 is larger then -0.7. Through this comparison, the six pixels obtain similarity indices from a class which they actually belong to, and therefore are going to be correctly classified. After the window moves to the last position (5, 5), all pixels are assigned the largest similarity indices from the class they really belong to. The edge effect is automatically eliminated during the process in this artificial example.

Classification Scenarios

In this section, we describe three classification scenarios and compare the results generated by the new approach and the traditional method.

In all three scenarios, three textural measures were used, i.e., *mean, standard deviation (std)*, and *entropy*. They were computed using the following formula:

$$mean = \frac{1}{MN}\sum_{i=0}^{M-1}\sum_{j=0}^{N-1} P(i,j) \quad (1)$$

$$std = \sqrt{\frac{\sum_{i=0}^{M-1}\sum_{j=0}^{N-1}(P(i,j) - mean)^2}{MN - 1}} \quad (2)$$

$$entropy = -\sum_{i=0}^{M-1}\sum_{j=0}^{N-1} Q(i,j)\log|Q(i,j)|\;(Q(i,j) \neq 0) \quad (3)$$

$$\text{where } Q(i,j) = \frac{|P(i,j)^2|}{\sum_{i=0}^{M-1}\sum_{j=0}^{N-1} P(i,j)^2} \quad (4)$$

where M and N are the height and width of the moving window, and $P(i, j)$ is the pixel value at position (i, j) within the window.

The minimum-distance classifier and the maximum-likelihood classifier were used in in the first two scenarios, and the logistic regression was used in the last scenario. For the minimum-distance classifier, the distance d was calculated as: $d = \sqrt{(x - \bar{x})^2 + (y - \bar{y})^2 + (z - \bar{z})^2}$, where x, y, z are the mean, standard deviation, and entropy, respectively, calculated from the moving window, and $\bar{x}, \bar{y}, \bar{z}$ are the mean values of the three measures for a particular class. As in the worked example, the similarity index is the negative of the distance, i.e., $-d$. For the maximum-likelihood classifier, the similarity index in the new approach is the probability density of a multivariate normal distribution:

$$p(x) = (2\pi)^{-n/2}|\Sigma|^{-1/2}\;\exp(-(x - \mu)^t\Sigma^{-1}(x - \mu)/2) \quad (5)$$

where x is the vector comprising of the three textural measures, μ is the mean vector of textural measures, and Σ is the variance-covariance matrix of textural measures.

In all three scenarios, one hundred random textural samples for each class were collected to compile the statistics needed for the two classifiers.

Classification of an Artificial Image

In the first classification scenario, an artificial image was generated, which consisted of four subimages (Figure 3). Each subimage was of size of 100×100 pixels, generated from a Gaussian distribution with different parameters. The mean and standard deviation of each Gaussian distribution are presented in Table 1. Figure 3 also shows the probability density curves of the four distributions. It is apparent that there is considerable overlapping in the range of pixel values among the four subimages.

Figure 4 shows the per-pixel classified image using the maximum-likelihood classifier without using textural measures. One hundred training pixels were randomly selected for each class. The overall accuracy was 40.00 percent and the kappa coefficient was 21.34 percent. It was apparent that per-pixel spectral classification did not provide satisfactory results in this case. However, each subimage showed a distinctive textural pattern, which could be used to distinguish itself from other subimages. Figure 5

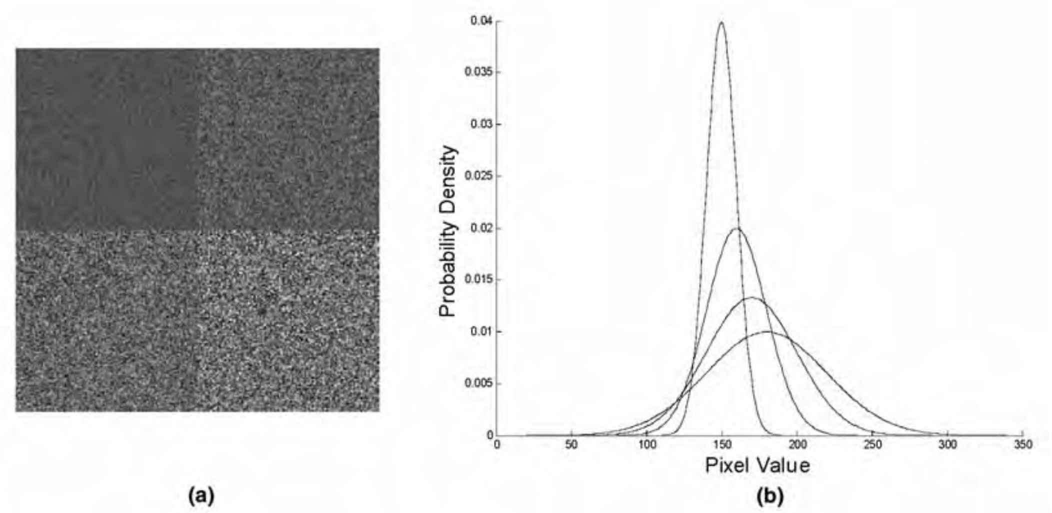

Figure 3. (a) An artificial image consisting of four subimages generated from different Gaussian distributions, and (b) Probability density curves of the four Gaussian distributions.

shows the classification accuracy of the image by the two approaches using both the minimum-distance classifier and the maximum classifier with window sizes varying from 3×3 to 33×33. In the case of the traditional approach, the accuracy increased first and then decreased steadily. The cutoff point of the window size was 9. This reflects the common dilemma in textural analysis. Small windows are associated with unstable textural measures while large windows are associated with large confusion along class boundaries. In comparison, the overall accuracy achieved by the new approach generally increased as the window size increased and leveled off when the window size was large enough (larger than 15×15). For the two smallest window sizes (3×3 and 5×5), the new approach achieved lower accuracy than the traditional approach when the maximum-likelihood classifier was used. It could be explained that small window size did not provide stable texture measures, causing the maximum-likelihood classifier unable to discriminate successfully among different classes. The minimum-distance classifier was less affected by this factor because it utilized only the means calculated from the samples while the maximum-likelihood classifier made use of not only the means but also the variances and covariances.

Figure 6 shows the classification results of the two approaches with a window size of 33 by 33 by the two classifiers. Some observations can be made. First, the traditional method left a strip of pixels along the border of the image unclassified using both classifiers. The width of the strip was approximately half the window size. The existence of the strip was due to the fact that windows centered upon the pixels in the strip had parts outside the image region. It was worth noting that the overall accuracy used here was based upon pixels not in the strip. For the new approach, all pixels were classified and the overall accuracy was based upon all pixels in the image. Second, the confusion along the class boundaries was much larger for the traditional approach than for the new approach. For the traditional approach, the confusion took place mainly along the horizontal middle part. In the middle left part, pixels tended to be misclassified as belonging to class B. This was because the mean and standard deviation of class B were between those of class A and class C, and a window along the boundary of class A and C tended to have a mean

Table 1. Means and Standard Deviations of Four Gaussian Distributions Used to Generate Subimages as Shown in Figure 3a

Name	Position in Figure 3a	Mean	Standard Deviation
Class A	Top Left	150	10
Class B	Top Right	160	20
Class C	Bottom Left	170	30
Class D	Bottom Right	180	40

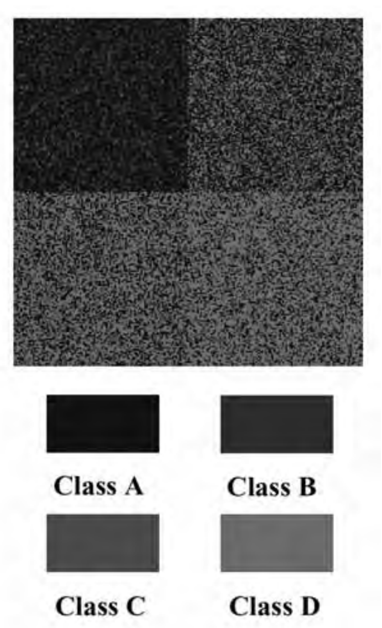

Figure 4. Per-pixel spectrally classified image using maximum-likelihood classifier.

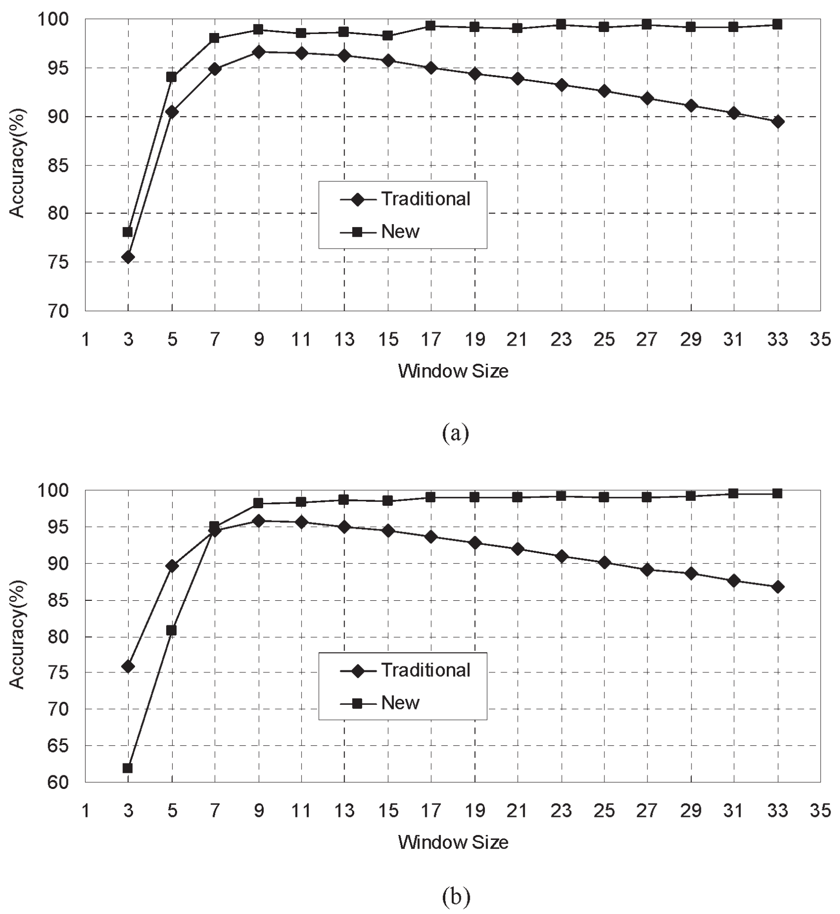

Figure 5. Classification accuracy with different window sizes for the artificial image by the traditional and the new methods: (a) using the minimum-distance classifier, and (b) using the maximum-likelihood classifier.

and standard deviation close to the averages of classes A and C, which were then similar to those of class B. In the middle right part, the confusion occurred for similar reasons. For the new approach, the confusion was much less and could be mainly attributed to the random fluctuations in the texture. Both classifiers achieved very satisfactory results using the new approach.

Classification of a Mosaic Image

A mosaic image (Figure 4) was created, which included six land-use samples: commercial, industrial, water, single-family, multifamily, and forest land uses. Each land -use sample was of size of 200 by 200 pixels (Figure 7). These land-use samples were taken from the panchromatic band of an Ikonos image, which covered part of metropolitan Atlanta, Georgia. The Ikonos image was taken on 29 December 2000. The coordinate system was Universal Transverse Mercator, Zone 16. The datum was WGS84.

Figure 8a shows the overall classification accuracy by the two approaches using the minimum-distance classifier. Because of the wide variation within each class, the window size began at 17 × 17. For the traditional method, the overall accuracy increased as the window size increased, reaching a maximum of about 82 percent at window size of 67 × 67, then dropped gradually by a small amount as window size further increased. For the new approach, the overall accuracy generally increased as the window size increased until it leveled off. There were only a few minor exceptions, which deviated from the trend only by a negligible amount. The new approach achieved higher accuracy than the traditional method irrespective of the window size used.

Figure 8b presents the overall classification accuracy by the two approaches using the maximum-likelihood classifier. When the window size was less than 55 × 55, the traditional approach produced slightly higher accuracy than the new approach. This result was different from that obtained using the minimum-distance classifier. It could be explained that small window sizes do not provide stable texture measures, causing the maximum-likelihood classifier unable to discriminate successfully among different classes. As a result, the new approach yielded lower accuracy than the traditional method. When the window size was larger than 55 × 55, the traditional approach yielded lower and lower accuracy as the window size increased whereas for the new approach, the overall accuracy kept increasing until it leveled off. When the window size was large enough (larger than 55 × 55) to generate stable measures, the maximum-likelihood classifier using the traditional moving window method achieved lower accuracy than using the new approach.

Figure 9 shows the classified images for a window size of 85 × 85. For both classifiers, we see that the new

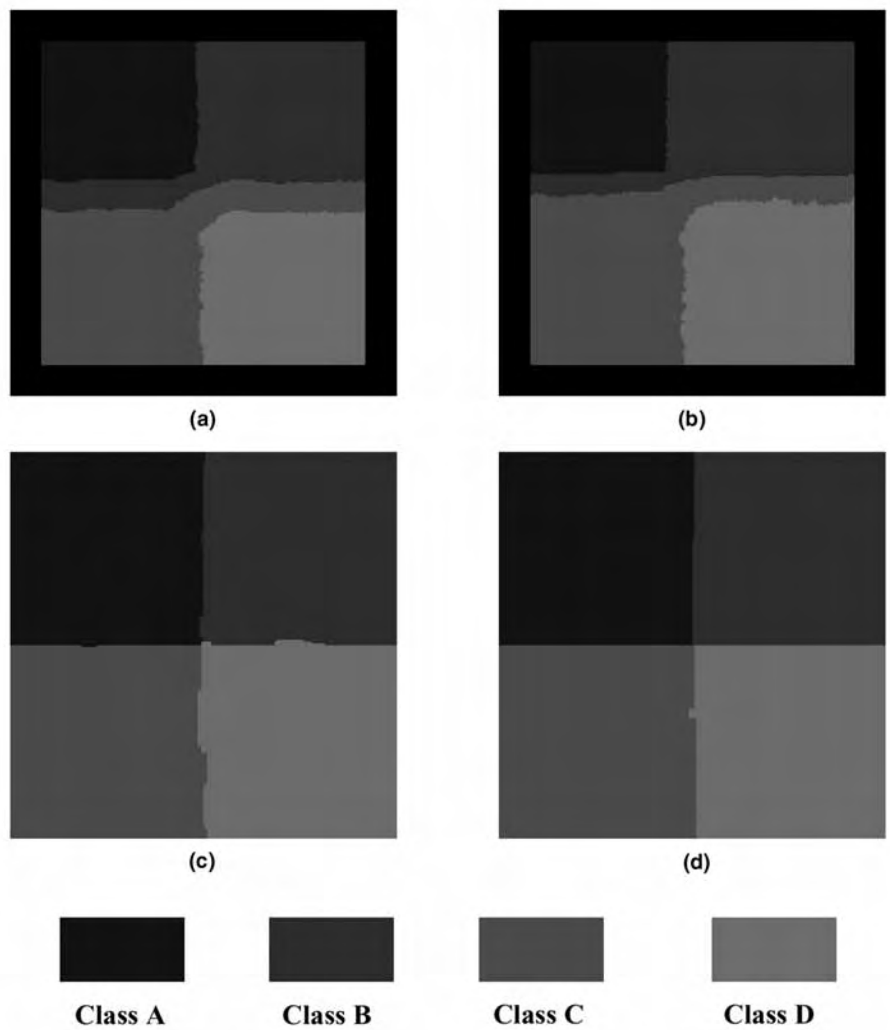

Figure 6. Classified results of the artificial image with a window size of 33 × 33: (a) the by minimum-distance classifier using the traditional method, (b) by maximum-likelihood classifier using the traditional method, (c) by minimum-distance classifier using the new method, and (d) by maximum-likelihood classifier using the new method.

approach reduced edge effects substantially. The edges between water and forest, water and industrial land-use, multifamily and forestland uses were clear by the new approach. With the maximum likelihood classifier, the boundaries between all classes were very close to the true boundaries using the new approach. Some errors arose, which could be ascribed to the considerable variation within each class shown in the mosaic image.

For the new approach, the smoothing effect was clear in both cases. Some small isolated clusters of pixels, present in the two images by the traditional method, were replaced with surrounding large classes. This smoothing effect was caused by the way the new approach utilized the textural information in the moving window. The small isolated clusters were large deviations from the surrounding pixels in terms of textural patterns they presented. An entire small cluster could be removed if its separate parts were removed by many neighboring moving windows using the criterion of highest similarity index. The smoothing effect was generally preferred because the smoothed map would easily be converted into areal units in vector format in subsequent analysis. In many traditional post-classification processing, a majority operation is applied to reduce the salt-and-pepper pattern and to obtain a smoothed map.

Identification of Non-agricultural Land-use by Logistic Regression

In the third scenario, an Ikonos image, acquired on 18 May 2001, covering part of rural northeastern Alabama was used. The projection was Universal Transverse Mercator, Zone 16. The datum was WGS84. A subset of the image (Figure 10) was extracted (600 × 300 pixels) and the subset contained two types of land-covers, agricultural land-use, and non-agricultural land-use. The agricultural land had a smooth pattern while the non-agricultural land had a rough and coarse pattern. The purpose of this experiment was to delineate the area of non-agricultural land-use from agricultural land-use. In the first two scenarios, the shape of the subimages matched the shape of the window, which might help to achieve favorable results. In this scenario, the class boundaries were irregular.

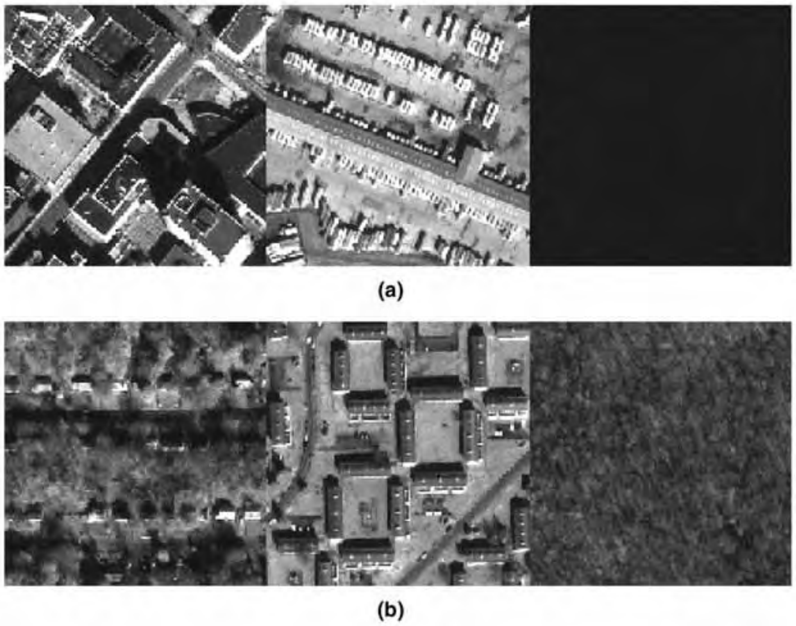

Figure 7. Mosaic image of six land use classes from the panchromatic band of an Ikonos image of Atlanta, Georgia: (a) commercial, industrial, and water, and (b) single-family, multifamily, and forest.

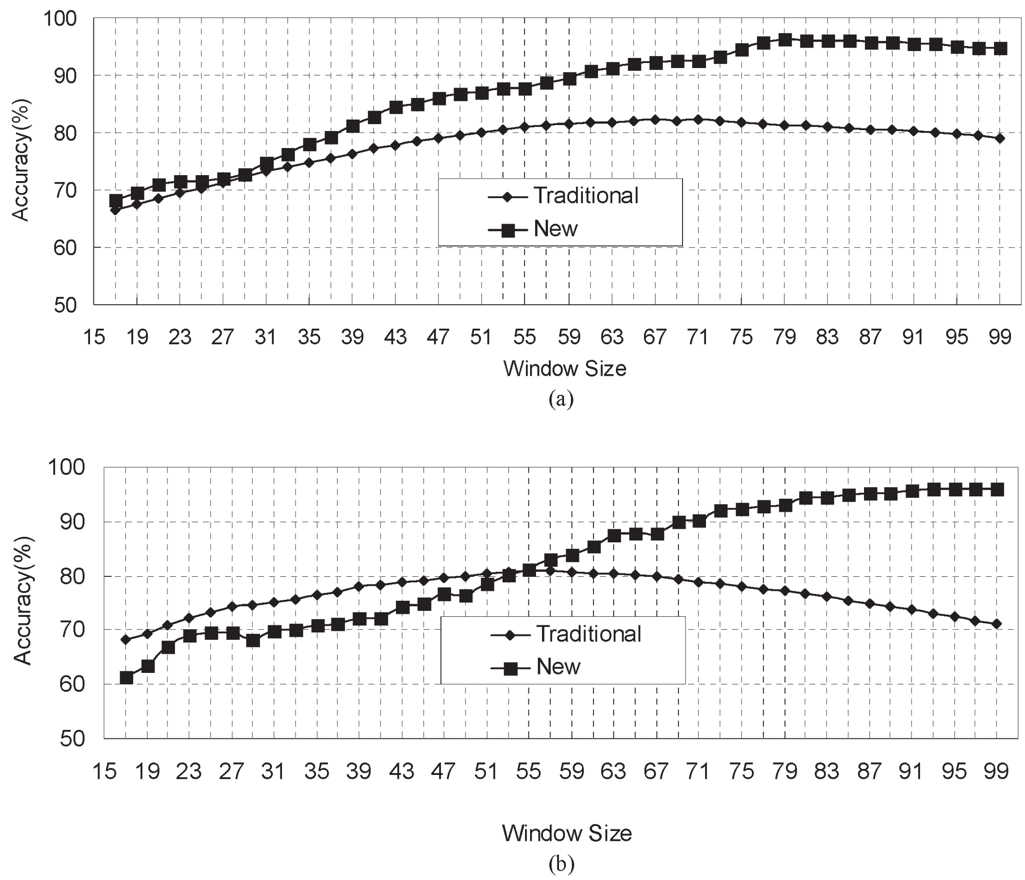

Figure 8. Classification accuracy with different window sizes for the artificial image by the traditional and the new methods using (a) the minimum-distance classifier, and (b) the maximum-likelihood classifier.

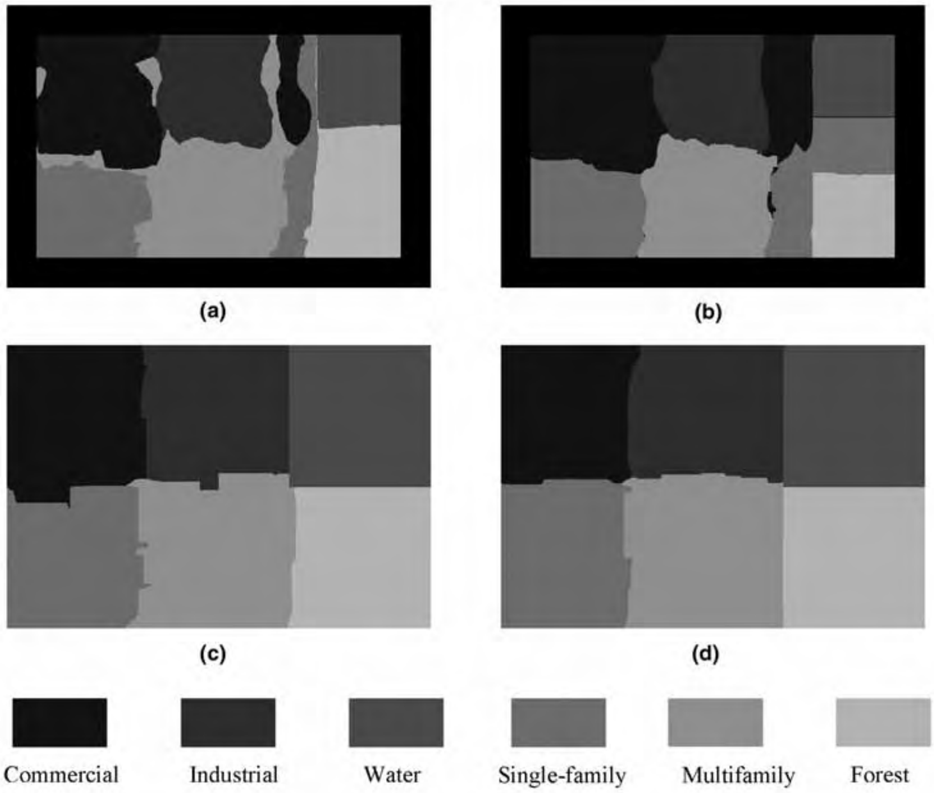

Figure 9. Classified results of the mosaic image with a window size of 85 $\times$ 85: (a) the by minimum-distance classifier using the traditional method, (b) by maximum-likelihood classifier using the traditional method, (c) by minimum-distance classifier using the new method, and (d) by maximum-likelihood classifier using the new method.

In this experiment, we used logistic regression (McCullagh and Nelder, 1989; Pampel, 2000) to distinguish between the two types of land-uses. Logistic regression is a useful tool when the dependent variable is dichotomous where the ordinary least squares regression is inappropriate. In logistic regression, the logit, which is the logarithm of the odds of an event (the ratio of the probability that an event occurs to the probability that it fails to occur), is treated as a latent variable and assumed to have a linear relationship with the input data:

$$\text{logit} = \log \frac{p}{1-p} = a + \vec{b}^T \vec{x} \tag{6}$$

so that we have:

$$p = \frac{\exp(a + \vec{b}^T \vec{x})}{1 + \exp(a + \vec{b}^T \vec{x})} \tag{7}$$

where a is a constant, $\vec{b}$ is the parameter vector, and $\vec{x}$ is the input vector, comprising of the three textural measures in this experiment. Based on training data, maximum-likelihood estimates of the parameters (a and $\vec{b}$) in the above equation can be obtained through an iterative process by the Newton-Raphson algorithm (McCullagh and Nelder, 1989; Pampel, 2000). The parameters can then be used to compute the probability of an event. Logistic regression has been successfully applied to map one particular type of phenomenon on an entire image such as the detection of burned scars (Pu and Gong, 2004) and the delineation of an exotic, invasive plant in Florida (Pearlstine *et al.*, 2005).

In this experiment, the non-agricultural class was treated as the event. So the probability of 1 was indicative of complete non-agricultural texture and the probability of 0 was indicative of complete agricultural texture. The

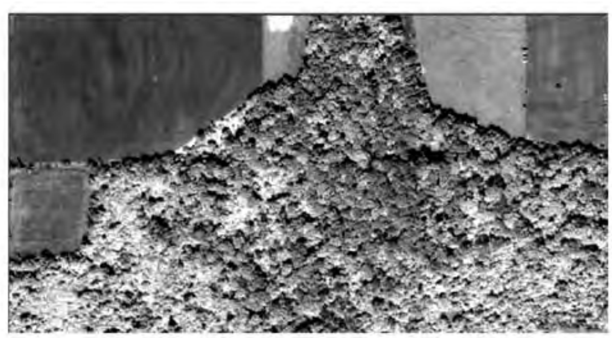

Figure 10. A subset of Ikonos panchromatic band with agricultural and non-agricultural land-uses.

similarity index was: p−1 if p >= 0.5 or −p if p < 0.5. The value of 0.5 was used as the cutoff point. Zero is the largest possible similarity index. This similarity index was the negative of distance in terms of probability.

Figure 11 plots the overall accuracy using the two approaches with window sizes varying from 17 × 17 to 51 × 51. As in previous scenarios, the new approach achieved higher accuracy over the traditional method. As the window size increased, the traditional method generally produced lower and lower accuracy whereas the accuracy by the new approach increased until it leveled off.

The classified images for the non-agricultural land use with the window size of 33 × 33 are shown in Figure 12. We see that for the traditional method, the commission errors largely occurred along the entire boundary between the agricultural and non-agricultural land uses, with some commission errors occurring as one small isolated clump. For the new method, the isolated small cluster of pixels was gone because of the smoothing effect discussed above. For the new method, the commission errors largely occurred on the top-middle part of the image. A close examination of the top-middle part of the image revealed that there were some bright pixels standing out from surrounding pixels in the agricultural land-use. This large anomaly might yield textural measures that were close to those of non-agricultural land-use, thus causing errors. For the traditional method, the omission errors occurred as four small clusters in the image (the pixels along the border were not counted). But three clusters were gone in the classified image by the new approach due to the smoothing effect. The new approach produced some small omission errors along the boundary.

Two computational considerations are noted here if logistic regression is used in this application as the basis for delineating dichotomous land-covers. First, the maximum-likelihood estimates do not always exist for logistic regression (Albert and Anderson, 1984; Santner and Duffy, 1986). In that case, the logistic model is questionable and should not be used. In our experiments, we could not find a convergence when the window size was larger than 51 × 51. Although popular statistical packages usually continue the process despite the failure to achieve convergence, the model, if used, may give unexpected results for both the traditional and the new methods.

Second, if the logit values are large enough (say larger than 50), the probability we get from $\frac{\exp(\text{logit})}{1 + \exp(\text{logit})}$ will always be 1 due to the precision limits in the computer for two different logit values even when there is a noticeable difference between them. The same is true when the logit is too small, and we will always get a probability of 0. As a result, a pixel along the boundary may be assigned the largest similarity index of zero when most of the moving window is agricultural and get the same largest similarity index of zero when most of the moving window is non-agricultural. In this case, the pixel has the chance of getting two maximum indices from two different categories and the order in which the pixel gets the indices affects the results. Since the probability increases monotonously as logit increases, this problem is eliminated if we compare the logit values directly when two logit values have the same sign. When two logits have different signs, we only need to compare the sum of the two logits with zero. The logit generally does not exceed the precision limits in the computer and can be compared reliably.

Discussion

From the above experiments, we show that the new approach has the following characteristics. First, the new approach consistently achieved higher accuracy with slight fluctuations until it leveled off, whereas the accuracy of the traditional approach generally decreased with increasing window size after the window size passed a threshold. Second, the new approach is capable of classifying border pixels, while the traditional method left a strip of border pixels unprocessed. Third, the new approach has a smoothing effect. Small isolated clusters, present in classified images by the traditional method, tended to be eliminated in classified images by the new approach. Fourth, the side length of the window could be an even number in the new approach because it does not use the concept of the center of the window, whereas in the traditional approach, the window size was usually odd to make sure the center pixel was the exact center.

For the new approach to be effective, the following requirements should be met. First, training samples should be representative as in any supervised classification scheme. Second, the texture measures used to determine class membership should be able to discriminate between homogenous samples and samples including more than one land-cover classes. This is important because the underlying assumption of the new approach is that texture containing mixed classes is dissimilar to texture containing one single class. If mixed texture yields a similarity index higher than that of homogeneous texture, errors will arise along class

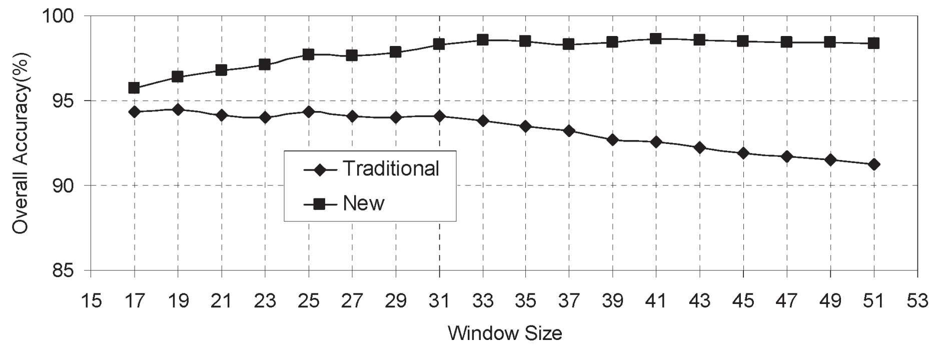

Figure 11. Overall classification accuracy using logistic regression.

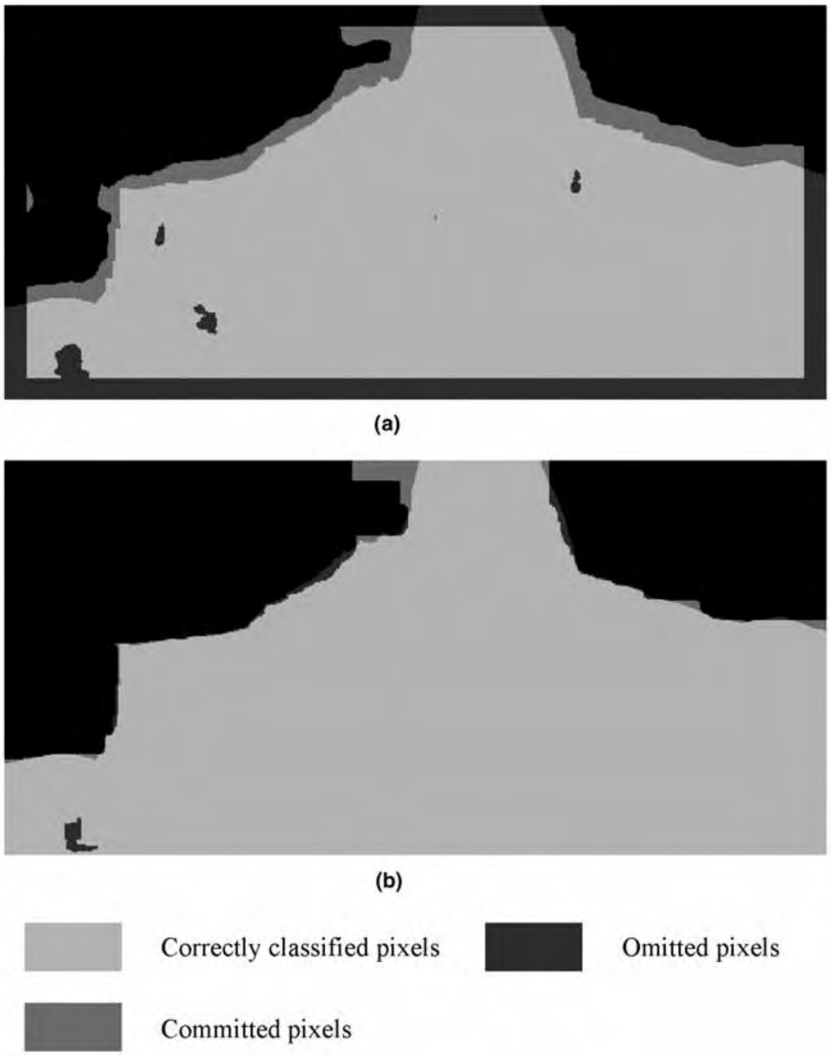

Figure 12. Classified image overlaid on the reference map for non-agricultural land-use with a window size of 33 × 33: (a) by the traditional method, and (b) by the new method.

boundaries because part of pixels in the mixed texture will be misclassified. Third, similarity index should be comparable among different windows, such as the probability density in the maximum-likelihood classifier, and the negative or the reverse of the distance in the minimum-distance classifier used in this study. In comparison, if linear discriminant analysis is used, the discriminant score should not be used as the similarity index, but rather the probability values derived from the discriminant scores should be used because the linear discriminant scores are not comparable among different observations while probability values are (Tatsuoka and Lohnes, 1988, p. 369).

In this paper, we carried out the experiments on only the panchromatic band of Ikonos images. The proposed method can easily be extended to multi-spectral imagery, where the similarity index can be calculated based on textural measures obtained from multiple bands. The complexity will also be greatly increased as the dimension increases. The proposed approach could easily work together with other textural measures and classifiers.

The new approach is not a panacea. For pixels that have no chance of entirely falling in a window containing only one type of texture, the edge issues tend to persist and the pixels tend to be misclassified. This happens when the class boundaries are too complex or the land-cover polygons are smaller than the window size used. This problem is inherent to regularly shaped windows. No single one geometric shaped window provides universally best results for all boundary types. Although dynamic windows with changing shape and size according to local structures had been suggested as a possible solution (Hodgson, 1998), the irregularity of the window shapes and sizes will make comparisons of their textural measures inconsistent and unreliable, leading to unexpected results and difficult interpretation. When there are a large number of classes in an image, particularly in large high-resolution images, the class polygon size varies substantially from one class to another class and the probability of errors may increase substantially with the increase in the number of classes.

Conclusions

This paper proposes a new approach to reducing the edge effects in image classification. In the new approach, all pixels in a moving window make use of the textural information instead of only the center pixel as in the traditional moving window method. Results from three classification scenarios, including the classification of an artificial image, a mosaic image and a natural scene, show that the new approach generally produced higher accuracy with increasing window size and was much less affected by edge issues than the traditional moving window method. The new approach yielded satisfactory results as long as the window size does not exceed the size of the land-cover polygons. More experiments with more complex class boundaries and different textural measures should help in revealing the best combination of textural measures and classifiers for this approach to reduce edge effects.

Acknowledgments

This research was supported by a dissertation improvement grant from the National Science Foundation under Grant No. 0602111 and a research grant from NASA Intelligent Systems research grant program under Grant No. NAS-2-37143.

References

Albert, A., and J.A. Anderson, 1984. On the existence of maximum likelihood estimates in logistic regression models, *Biometrika*, 71(1):1–10.

Chen, D., D.A. Stow, and P. Gong, 2004. Examining the effect of spatial resolution and texture window size on classification accuracy: An urban environment case, *International Journal of Remote Sensing*, 25(11):2177–2192.

Ferro, C.J.S., and T.A. Warner, 2002. Scale and texture in digital image classification, *Photogrammetric Engineering & Remote Sensing*, 68(1):51–63.

Gong, P., 1994. Reducing boundary effects in a kernel-based classifier, *International Journal of Remote Sensing*, 15(5):1131–1139.

Gong, P., and P.J. Howarth, 1992. Frequency-based contextual classification and gray-level vector reduction for land-use identification, *Photogrammetric Engineering & Remote Sensing*, 58(4):423–437.

Gong, P., D.J. Marceau, and P.J. Howarth, 1992. A comparison of spatial feature extraction algorithms for land-use classification with SPOT HRV data, *Remote Sensing of Environment*, 40(2):137–151.

Haack, B., N. Bryant, and S. Adams, 1987. An assessment of Landsat MSS and TM data for urban and near-urban land-cover digital classification, *Remote Sensing of Environment*, 21(2):201–213.

Haralick, R.M., and L.G. Shapiro, 1985. Image segmentation techniques, *Computer Vision Graphics Image Process*, 29:100–132.

Hodgson, M.E., 1998. What size window for image classification? A cognitive perspective, *Photogrammetric Engineering & Remote Sensing*, 64(8):797–807.

Hsu, S., 1978. Texture-tone analysis for automated land-use mapping, *Photogrammetric Engineering & Remote Sensing*, 44(11):1393–1404.

Hu, X., V. Tao, and B. Prenzel, 2005. Automatic segmentation of high-resolution satellite imagery by integrating texture, intensity, and color features, *Photogrammetric Engineering & Remote Sensing*, 71(12):1399–1406.

Jensen, J.R., 2005. *Introductory Digital Image Processing*, Third edition, Prentice Hall, Upper Saddle River, New Jersey.

Lucieer, A., and A. Stein, 2005. Texture-based landform segmentation of LiDAR imagery, *International Journal of Applied Earth Observation and Geoinformation*, 6(3–4):261–270.

Lucieer, A., A. Stein, and P. Fisher, 2005. Multivariate texture-based segmentation of remotely sensed imagery for extraction of objects and their uncertainty, *International Journal of Remote Sensing*, 26(14):2917–2936.

Maillard, P., 2003. Comparing texture analysis methods through classification, *Photogrammetric Engineering & Remote Sensing*, 69(4):357–367.

Marceau, D.J., D.P.J. Howarth, J.M. Dubois, and D.J. Gratton, 1990. Evaluation of the grey-level co-occurrence matrix method for landcover classification using SPOT imagery, *IEEE Transactions on Geoscience and Remote Sensing*, 28(4):513–519.

McCullagh, P., and J.A. Nelder, 1989. *Generalized Linear Models*, Chapman and Hall, New York.

Nellis, M.D., and J.M. Briggs, 1989. The effect of spatial scale on Konza landscape classification using textural analysis, *Landscape Ecology*, 2(2):93–100.

Ojala, T., and M. Pietikainen, 1999. Unsupervised texture segmentation using feature distributions, *Pattern Recognition*, 32:477–486.

Ojala, T., M. Pietikainen, and T. Maenpaa 2002. Multiresoluton gray-scale and rotation invariant texture classification with local binary patterns, *IEEE Transactions on Pattern Analysis and Machine Intelligence*, 24(7):971–987.

Pampel, F.C., 2000. *Logistic Regression: A Primer*, SAGE Publications, Thousand Oaks, California.

Pearlstine, L., K. M. Portier, and S.E. Smith, 2005. Textural discrimination of an invasive plant, *Schinus terebinthifolius*, from low altitude aerial digital imagery, *Photogrammetric Engineering & Remote Sensing*, 71(3):289–298.

Pu, R., and P. Gong, 2004. Determination of burnt scars using logistic regression and neural network techniques from a single post-fire landsat 7 ETM+ image, *Photogrammetric Engineering & Remote Sensing*, 70(7):841–850.

Santner, T.J., and D.E. Duffy, 1986. A note on A. Albert and J. A. Anderson's conditions for the existence of maximum likelihood estimates in logistic regression models, *Biometrika*, 73(3):755–758.

St-Onge, B.A., and F. Cavayas, 1995. Estimating forest stand structure from high resolution imagery using the directional variogram, *International Journal of Remote Sensing*, 16(11):1999–2021.

Tatsuoka, M.M., and P.R. Lohnes, 1988. *Multivariate Analysis*, Macmillan Publishing Company, New York.

Warner, T.A., and K. Steinmaus, 2005. Spatial classification of orchards and vineyards with high spatial resolution panchromatic imagery, *Photogrammetric Engineering & Remote Sensing*, 71(2):179–187.

(Received 17 January 2006; accepted 01 May 2006; revised 14 September 2006)